with ten or more layers one can design a cloak that is practically invisible. Furthermore, it is shown that the bandwidth of the Schurig cloak can indeed be increased by up to a factor of 2.5, by optimizing the cloak layer parameters, while maintaining the same minimal value of the total scattered width. Finally, it is demonstrated that losses in the cloak increase the total scattering width, in other words, reduce the invisibility gain. However, for values of around $\gamma = 10^{-3} f_0$ the invisibility gain of the optimized cloak is still roughly equal to the invisibility of the Schurig cloak with no losses.

REFERENCES

[1] L. S. Dollin, "On the possibility of comparison of three-dimensional electromagnetic systems with nonuniform anisotropic filling," *Izv. VUZov Radiofizika*, vol. 4, no. 5, pp. 964–967, 1961.

[2] M. Kerker, "Invisible bodies," *J. Opt. Soc. Am.*, vol. 65, pp. 376–379, Apr. 1975.

[3] N. G. Alexopoulos and N. K. Uzunoglu, "Electromagnetic scattering from active objects: Invisible scatterers," *Appl. Opt.*, vol. 17, pp. 235–239, Jan. 1978.

[4] P. S. Kildal, A. A. Kishk, and A. Tengs, "Reduction of forward scattering from cylindrical objects using hard surfaces," *IEEE Trans. Antennas Propag.*, vol. AP-44, pp. 1509–1520, Nov. 1996.

[5] J. B. Pendry, D. Schurig, and D. R. Smith, "Controlling electromagnetic fields," *Science*, vol. 312, pp. 1780–1782, Jun. 2006.

[6] D. Schurig, J. J. Mock, B. J. Justice, S. A. Cummer, J. B. Pendry, A. F. Starr, and D. R. Smith, "Metamaterial electromagnetic cloak at microwave frequencies," *Science*, vol. 314, pp. 977–980, Nov. 2006.

[7] W. Cai, U. K. Chettiar, A. V. Kildishev, and V. M. Shalaev, "Optical cloaking with non-magnetic metamaterials," *Nature Photon.*, vol. 1, pp. 224–227, Apr. 2007.

[8] B. Ivsic, Z. Sipus, and S. Hrabar, "Analysis of uniaxial multilayer cylinders used for invisible cloak realization," *IEEE Trans. Antennas Propag.*, vol. AP-57, pp. 1521–1527, May 2009.

[9] E. F. Knott, J. F. Shaeffer, and M. T. Tuley, *Radar Cross Section*. New York: SciTech Publishing, 2004.

[10] S. Hrabar, , N. Engheta and R. Ziolkowsky, Eds., "Waveguide experiments to characterize the properties of SNG and DNG metamaterials," in *Metamaterials: Physics and Engineering Explorations*. Hoboken/Piscataway, NJ: Wiley and IEEE, 2006, ch. 3.

[11] S. Hrabar, L. Benic, and J. Bartolic, "Simple experimental determination of complex permittivity or complex permeability of SNG metamaterials," in *Proc. 36th Eur. Microwave Conf.*, Manchester, U.K., Sep. 2006, pp. 1395–1398.

[12] B.-I. Popa and S. A. Cummer, "Cloaking with optimized homogeneous anisotropic layers," *Phys. Rev. A*, vol. 79, no. 023806, 2009.

[13] J. Robinson and Y. Rahmat-Samii, "Particle swarm optimization in electromagnetics," *IEEE Trans. Antennas Propag.*, vol. 52, no. 2, pp. 397–407, Feb. 2004.

[14] D. W. Boeringer and D. H. Werner, "Particle swarm optimization versus genetic algorithms for phased array synthesis," *IEEE Trans. Antennas Propag.*, vol. 52, no. 3, pp. 771–778, Mar. 2004.

[15] J. Kennedy and R. Mendes, "Neighborhood topologies in fully informed and best-of-neighborhood particle swarms," *IEEE Trans. Syst. Man, Cybern. Part C*, vol. 35, no. 4, pp. 515–519, Jul. 2006.

[16] P. Demarcke, H. Rogier, R. Goossens, and P. De Jaeger, "Beamforming in the presence of mutual coupling based on constrained particle swarm optimization," *IEEE Trans. Antennas Propag.*, vol. 57, no. 6, pp. 1655–1666, Jun. 2009.

[17] J. J. Liang, K. Qin, P. N. Suganthan, and S. Baskar, "Comprehensive learning particle swarm optimizer for global optimization of multimodal functions," *IEEE Trans. Evol. Comput.*, vol. 10, no. 3, pp. 281–295, Jun. 2006.

[18] H. Wu, J. Geng, R. Jin, J. Qiu, W. Liu, J. Chen, and S. Liu, "An improved comprehensive learning particle swarm optimization and its application to the semiautomatic design of antennas," *IEEE Trans. Antennas Propag.*, vol. 57, no. 10, pp. 3018–3028, Oct. 2009.

[19] T. Komljenovic, R. Sauleau, Z. Sipus, and L. L. Coq, "Layered circular-cylindrical dielectric lens antennas—Synthesis and height reduction technique," *IEEE Trans. Antennas Propag.*, accepted for publication.

A Hybrid Optimization Algorithm and Its Application for Conformal Array Pattern Synthesis

Wen Tao Li, Xiao Wei Shi, Yong Qiang Hei, Shu Fang Liu, and Jiang Zhu

***Abstract*—Investigations on conformal phased array pattern synthesis using a novel hybrid evolutionary algorithm are presented. First, in order to overcome the drawbacks of the standard genetic algorithm (GA) and the particle swarm optimization (PSO), an improved genetic algorithm (IGA) and an improved particle swarm optimization (IPSO) algorithm are proposed by introducing novel mechanisms. Then, inspired by the idea of grafting in botany, a hybrid algorithm called HIGAPSO is proposed, which combines IGA and IPSO to take advantages of both methods. After that, a spherical array antenna using wide-band stacked patch antenna elements is selected as a synthesis example to illustrate the power of HIGAPSO in solving realistic optimization problems. Finally, HIGAPSO is used to optimize the amplitude of the element current excitation of the spherical conformal array. Experimental results show that the hybrid algorithm is superior to GAs and PSOs when applied to both the classical test function and the practical problem of conformal antenna array synthesis.**

***Index Terms*—Array synthesis, conformal antenna array, genetic algorithm, particle swarm optimization.**

I. INTRODUCTION

Conformal antenna arrays have attracted more and more attention in many applications where planar arrays or reflector antennas have definite drawbacks [1]–[3]. This is because conformal antenna arrays have advantages of visual unobtrusiveness, non-interference with the aerodynamic performance and antenna performance. Nowadays, many technologies have been proposed for their analysis and synthesis [4]–[7]. However, low side-lobe array pattern synthesis techniques developed for linear and planar arrays do not work well with conformal arrays, since, if the array is conformal to a curved surface, the radiating elements are directed in different directions, posing unique challenges in the synthesis of antenna arrays. Therefore, it is desirable to develop an algorithm which is robust and has excellent global optimization performance and fast convergence speed in the antenna synthesis field. Although great progress has been made in the development of the evolutionary computation recently [8]–[11] in such a way that they are more robust and efficient to solve real-world problems when compared with traditional computation systems, they show limitations in solving conformal array synthesis problems.

Since both PSO and GA algorithms work with a population of solutions, recently some attempts have been made to combine them, but with a weak integration of these two methods [12]–[14]. In this communication, we addressed this problem from a different perspective.

Manuscript received May 12, 2009; revised February 04, 2010; accepted February 05, 2010. Date of publication May 18, 2010; date of current version October 06, 2010. This work was supported by the National Science Foundation of China under Grant 60571057.

W. T. Li, X. W. Shi, and S. F. Liu are with the National Key Laboratory of Science and Technology on Antennas and Microwaves, Department of Electronic Engineering, Xidian University, Xi'an 710071, China (e-mail: wtli@mail.xidian.edu.cn).

Y. Q. Hei is with the State Key Laboratory of ISN, Xidian University, Xi'an 710071, China (e-mail: yqhei@mail.xidian.edu.cn).

J. Zhu is with the Edward S. Rogers Sr. Department of Electrical and Computer Engineering, University of Toronto, Toronto, ON M5S 3G4, Canada (e-mail: jiangzhu@waves.utoronto.ca).

Color versions of one or more of the figures in this communication are available online at http://ieeexplore.ieee.org.

Digital Object Identifier 10.1109/TAP.2010.2050425

Firstly, two new evolutionary algorithms, IGA and IPSO derive from GA and PSO by introducing some new mechanisms. Then, they are tightly combined into a new hybrid algorithm called HIGAPSO, in which the grafting principle is employed to take full advantages of these methods. Our current proposal is an improved version of the algorithm reported in [18], in which the novel mechanisms and the grafting idea are introduced to improve the the convergence speed and the optimum search ability. After that, a typical benchmark function is presented to validate the proposed algorithm. Furthermore, a stacked Minkowski fractal microstrip antenna is used to design the spherical conformal array. In this example, the proposed algorithm has demonstrated its capability to reduce the side-lobe levels by optimizing the element amplitude weights.

The remainder of the communication is organized as follows: Section II presents the detailed architecture of the proposed hybrid algorithm. The low side-lobe pattern synthesis of a spherical array based on the proposed algorithm is given in Section III, while Section IV concludes this communication.

II. Hybrid of IGA and IPSO

Consider a global optimization problem:

$$\begin{aligned} &\min f(x) = f(x_1, x_2, \cdots x_n) \\ S.t. \quad & x_i^{\min} \le x_i \le x_i^{\max} \qquad (i = 1, 2, \cdots n) \end{aligned} \tag{1}$$

where n is the number of the optimized variables, $x_i^{\min}$ and $x_i^{\max}$ are the upper and lower bounds of x_i respectively.

In the following part, IGA and IPSO will be introduced, followed by the details of the proposed hybrid algorithm. After that a typical benchmark function is used to demonstrate the proposed hybrid algorithm.

A. Improved Genetic Algorithm

1) Crossover: In natural biological evolution, several offspring may be generated by the two parents after crossover and inevitably a competition relationship exists among those offspring produced by the same parents. Motivated by that, new crossover operator introducing competition manipulation among the offspring of the same parent is adopted in IGA. Now define the two parent chromosomes as $\vec{a}_s = [x_1^s \; x_2^s \; \cdots \; x_n^s]$ and $\vec{a}_t = [x_1^t \; x_2^t \; \cdots \; x_n^t]$, respectively, then the corresponding four offspring chromosomes are obtained according to:

$$\begin{aligned} \vec{b}_1 &= \begin{bmatrix} b_1^1 & b_2^1 & \cdots & b_n^1 \end{bmatrix} \\ &= w(\vec{a}_s + \vec{a}_t)/2 + (1-w)\max(\vec{a}_s, \vec{a}_t) \end{aligned} \tag{2}$$

$$\begin{aligned} \vec{b}_2 &= \begin{bmatrix} b_1^2 & b_2^2 & \cdots & b_n^2 \end{bmatrix} \\ &= (1-w)\min(\vec{a}_s, \vec{a}_t) + w(\vec{a}_s + \vec{a}_t)/2 \end{aligned} \tag{3}$$

$$\begin{aligned} \vec{b}_3 &= \begin{bmatrix} b_1^3 & b_2^3 & \cdots & b_n^3 \end{bmatrix} \\ &= \vec{a}_{\max}(1-w) + \max(\vec{a}_s, \vec{a}_t)w \end{aligned} \tag{4}$$

$$\begin{aligned} \vec{b}_4 &= \begin{bmatrix} b_1^4 & b_2^4 & \cdots & b_n^4 \end{bmatrix} \\ &= \vec{a}_{\min}(1-w) + \min(\vec{a}_s, \vec{a}_t)w \end{aligned} \tag{5}$$

$$\vec{a}_{\max} = [x_1^{\max} \quad x_2^{\max} \quad \cdots \quad x_n^{\max}] \tag{6}$$

$$\vec{a}_{\min} = \begin{bmatrix} x_1^{\min} & x_2^{\min} & \cdots & x_n^{\min} \end{bmatrix} \tag{7}$$

where $w \in [0, 1]$, $\max(\vec{a}_s, \vec{a}_t)$ denotes the vector with each element obtained by taking the maximum among the corresponding element of $\vec{a}_s$ and $\vec{a}_t$. Inspired by survival of the fittest principle in Darwinian evolution theory, we choose the two offspring with better fitness values among $\{\vec{b}_1, \cdots, \vec{b}_4\}$ as the output of the crossover operation.

For our proposed crossover operator, (2) and (3) can be seen as the results of interpolation, which leads to offspring search in the domain between $\vec{a}_s$ and $\vec{a}_t$. While (4) and (5) can be regarded as the results of extrapolation, which results in offspring searching the rest of the domain. Then the potential offspring are capable of spreading over the entire domain. A similar crossover operator is presented in [15], however, certain search space is missed when compared with our scheme (see Appendix).

2) Mutation: To avoid overly fast converging to a local optimum domain, the offspring generated by crossover operation will undergo the mutation operation [16]. Define the original offspring and the mutated offspring as $\vec{x}$ and $\vec{x}' = (x_1 \; \cdots \; \overline{x}_k \; \cdots \; x_n)$, respectively. The randomly selected variable $\overline{x}_k$ for mutation is defined as

$$\overline{x}_k = x_k^L + \left(x_k^U - x_k^L\right) w \tag{8}$$

$$x_k^U = \min\left(x_k + \mu\left(x_k^{\max} - x_k^{\min}\right)/2, x_k^{\max}\right) \tag{9}$$

$$x_k^L = \max\left(x_k - \mu\left(x_k^{\max} - x_k^{\min}\right)/2, x_k^{\min}\right) \tag{10}$$

where $w \in [0, 1]$ and μ is determined by

$$\mu(\tau) = 1 - (\tau/T)^{[1-(\tau/T)]^b} \tag{11}$$

where T is the maximum number of iterations, τ is the current iteration number, and b is the shape parameter. From (11), it is discovered the advantage of such mutation operator is that at the initial stage of evolution, $\mu(\tau) \approx 1$, the mutation domain is large. However, in the later evolution when τ approaches to T, $\mu(\tau) \approx 0$, the mutation domain becomes small and the individuals search in a local domain.

B. Improved Particle Swarm Optimization

1) Exceeding Boundary Control: Particles are commonly found lying outside the boundaries of the solution space during the position updating process. For such cases, the general methods are either to take the boundary as the coordinate of the new particle, or to keep the coordinate of the particle unchanged but to assign a poor fitness value to the particle. However, either approach may reduce the diversity of the particle as well as the global search ability of the algorithm. To keep the diversity of the particles, a novel approach is proposed

$$\vec{v}_i(\tau)_{new} = -\frac{d}{D} \cdot \vec{v}_i(\tau) \tag{12}$$

where $\vec{v}_i(\tau)$ is the particle velocity, d is the distance between the particle and its violation boundary, and D is its variation range. The new velocity is determined by the violation distance, the variation range and the previous velocity, in such a way it can improve the diversity of the particles in the searching process and the global search ability of the algorithm.

2) Global Best Perturbation: PSO has been shown to converge rapidly at the initial stages of a global search, but slows down when the search is close to the global optimum. To this point, the global best perturbation operator is adopted in IPSO. In social society, the leader in a swarm can be always found to explore more regions in order to lead the swarm to achieve the target with a faster speed. Inspired by this behavior, the perturbation operation is applied to the global best particle on the basis of the extrapolation theory

$$\vec{p}_g(\tau) = \vec{p}_g(\tau) + e_d \cdot \vec{p}_g(\tau) \tag{13}$$

where $\vec{p}_g$ is the best global solution, e_d is the extrapolation coefficient defined as

$$e_d = 1 - (1 + r_d)e^{[1-(\tau/T)]} \tag{14}$$

r_d is the uniformly distributed random number in [0,1]. By means of (13) and (14), the stagnant global best particle can be activated again so the global best can be found with a much higher probability.

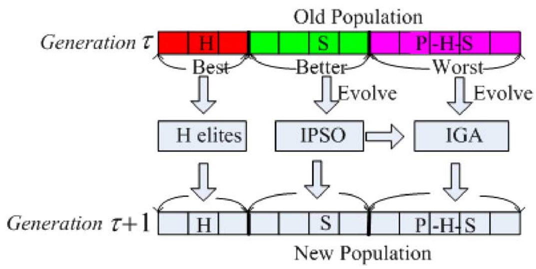

Fig. 1. Flow of key operations in HIGAPSO.

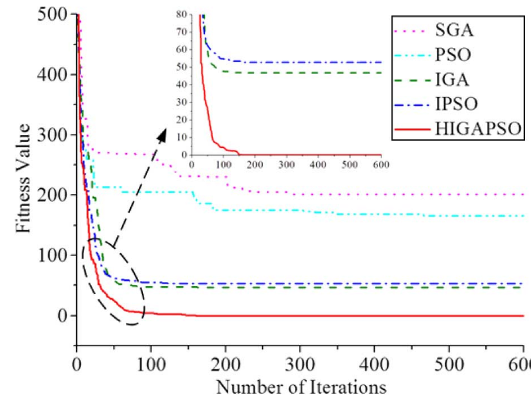

Fig. 2. The average best fitness results over 20 independent runs.

C. Hybrid Optimization Algorithm (HIGAPSO)

Inspired by the principle that grafting in botany can integrate the superiority of the two original branches, the proposed hybrid algorithm combines IGA with IPSO to take the advantages of both methods. In each generation, based on the fitness values, the population is firstly divided into three parts: the best individuals, the better individuals and the worst individuals. The best individuals are directly reproduced to the next generation; while the following better individuals are enhanced by IPSO to generate the corresponding individuals of next generation. Those IPSO-enhanced individuals regarded as the grafting population together with the rest individuals, are evolved with IGA to generate the remaining individuals of next generation. For clarity, the flow of key operations is illustrated in Fig. 1 with sequential steps of the algorithm given below.

Step 1) Randomly initialize a population of P individuals within the constraint range.

Step 2) Calculate the fitness of each individual from the fitness function, and then sort the individuals in ascending order according to their fitness values.

Step 3) Choose the top H individuals as the elites and directly reproduce them to the next generation.

Step 4) Apply IPSO strategy to the S better individuals and those IPSO-enhanced individuals are regarded as the grafting population.

Step 5) The rest $P-H-S$ individuals together with the IPSO-enhanced individuals, are evolved with IGA. Then the best $P-H-S$ individuals are selected as the remaining individuals of next generation.

Step 6) Combine the three parts together as the population of the new generation and calculate their fitness values. Choose the best one among all the individuals obtained so far as the global best.

Step 7) Repeat Steps 3 to 6 until a stopping criterion (i.e., a sufficiently good solution being discovered or a maximum number of generations being completed) is satisfied. The best scoring individual in the population is taken as the final solution.

In the proposed algorithm, the better individuals are evolved with IPSO instead of IGA. This is because compared with GA, PSO has the advantages of memory efficiency and cooperation between particles. Therefore, IPSO is more reasonable to take the task in guiding evolution. Besides, IPSO has good flexibility in controlling the balance between local and global exploration of the problem space, which can readily overcome the premature convergence of elite strategy in IGA. Then, the combination of these two optimization mechanisms, not only improves the diversity of the offspring, but also maintains the balance of global search and local search. Therefore, the search ability of the algorithm can be enhanced.

D. Preliminary Numerical Experiments

A typical test function is presented here to verify the efficiency of the hybrid algorithm. Algorithms of standard GA (SGA), IGA, PSO and IPSO are simulated for comparison.

The test functions is

$$f(x)=\sum_{i=1}^{30}\left[x_i^2-10\cos(2\pi x_i)+10\right],\quad x_i\in[-10,10]. \tag{15}$$

The function defined in (15) is known as Rastigrin function with a global minimum of zero at the origin. This is a tough multimodal optimization problem, because the global minimum is surrounded by a large number of local minima, making the search of global minimum without being stuck at one of these local minima extremely difficult.

The influence of parameters on the proposed algorithm has been investigated and we have found that the algorithm is sensitive to the population size and the percentage of S/P. Simulation results show that the optimum value of the population size is from $round(2n/3)$ to $round(7n/5)$ and the rational value of S/P changes from 0.18 to 0.35. For the test function, we choose population size $P=30$, the maximum number of iterations $T=600$, the number of elites $H=2$, crossover probability $p_c=0.8$, the mutation probability $p_m=0.02$ and the acceleration constant $c_1=c_2=2.0$. In IPSO, the number of population in each iteration is $S=0.2P$. The average best fitness results obtained from the five algorithms under test through 20 independent simulations are illustrated in Fig. 2. From the simulation results, it can be concluded that:

1) Either SGA or PSO can hardly achieve the ideal results especially for the high dimensional problems, which is due to their inherent defects of evolutionary mechanisms. It is exactly these defects that make the algorithm prematurely converged or easily trapped in a local optimum.
2) Compared with SGA and PSO, the IGA and IPSO can obtain better results. This fact accounts well for those improvements on SGA as well as PSO are indeed efficient to overcome the drawbacks of GA and PSO to some extent.
3) The HIGAPSO has the strongest local search ability and the fastest convergence speed among the five previously mentioned algorithms. This implies that IGA and IPSO can take the advantages of grafting idea in our hybrid algorithm; hence, a superior performance can be achieved by HIGAPSO.
4) As for the complexity, HIGAPSO is approximately the same as IGA or GA. Although additional complexity afford of IPSO is introduced, the evolutionary iterations can be reduced. Therefore, the complexity of HIGAPSO is comparable to IGA and GA.

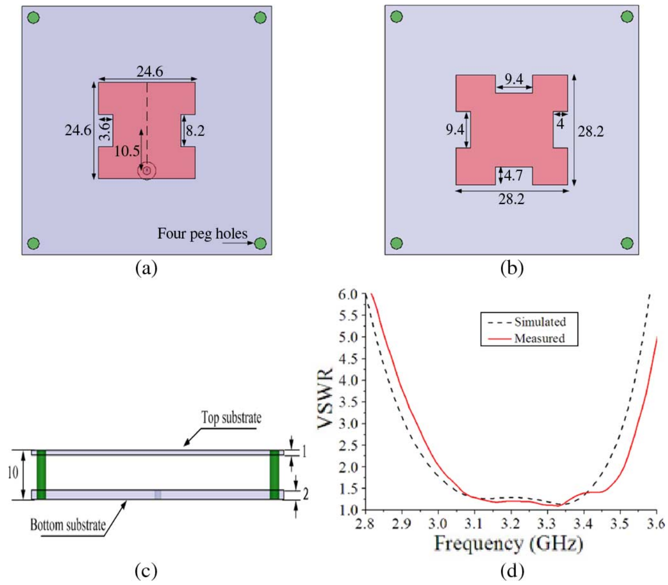

Fig. 3. Configuration of a coaxial-fed, stacked fractal patch antenna. (a) Top view of bottom layer. (b) Top view of top layer. (c) Side view. (All units are in mm). (d) Simulated and measured VSWR for the antenna.

III. Pattern Synthesis of a Conformal Antenna Array

A. Array Element Design

Microstrip patch antenna is extensively utilized as the array element for their low profile, light weight, and low cost. Besides, they can be easily made conformal. In this communication, a compact stacked antenna is designed to have a center frequency of 3.2 GHz and a bandwidth exceeding 12% for $\mathrm{VSWR} \leq 2$. The Ansoft HFSS 11.0 is employed to perform the design. The geometry of the fractal stacked array element antenna, along with its optimized dimensions, is shown in Fig. 3, which is fabricated on two layers with relative permittivity of 2.65. The top layer consists of a one order quasi-Minkowski fractal patch and has a dimension of $28.2 \times 28.2\ \mathrm{mm}^2$. The bottom layer consists of an H-shaped patch and has a dimension of $24.6 \times 24.6\ \mathrm{mm}^2$. The distance between the two layers is 7 mm. The antenna is fed by a standard SMA coaxial connector from the bottom. Compared with the regular rectangular patch antenna with dimensions of $27.1 \times 27.1\ \mathrm{mm}^2$ on the bottom layer and $31.3 \times 31.3\ \mathrm{mm}^2$ on the top layer, the sizes of our patches are reduced by 17.6% and 18.83% respectively. Thus, the mutual coupling can be reduced. The impedance bandwidth $(\mathrm{VSWR} \leq 2)$ is measured by Agilent N5230A network analyzer. From Fig. 3(d), it can be seen that the designed antenna covers from 3.0 to 3.51 GHz (15.67%) and the simulated result agrees with the measured one very well. Therefore, the designed antenna can fully satisfy with the design requirements.

B. Conformal Antenna Array Configuration

A half spherical array consisting of $N = 8$ concentric rings in the z-direction is investigated. The array is made up of a total number of 201 stacked fractal patch antennas on the sphere with radius $R = 500\ \mathrm{mm}$. Antennas are uniformly distributed along θ-direction (from $\theta = 0^\circ$ to $\theta = 60^\circ$) and φ-direction at approximately $0.65\lambda_0$. Assume the spherical coordinate of the mth $(m = 1, 2 \cdots, M_n)$ element on the nth concentric ring is $(R, \theta_n, \varphi_{mn})$ and the corresponding excitation current is $I_{mn} \exp j\psi_{mn}$, then the radiation pattern of the spherical array can be expressed as

$$FF(\theta,\varphi) = \sum_{n=1}^{N}\sum_{m=1}^{M_n} I_{mn} f_{mn}(\theta,\varphi) \times \mathrm{e}^{(jkR(\sin\theta\sin\theta_n\cos(\varphi-\varphi_{mn})+\cos\theta\cos\theta_n)+j\psi_{mn})} \quad (16)$$

where $f_{mn}(\theta,\varphi)$ is the individual element pattern and k is the free-space wave number. The excitation current phase ψ_{mn} can be calculated by:

$$\psi_{mn} = -kR\left[\sin\theta_0\sin\theta_n\cos(\varphi_0-\varphi_{mn}) + \cos\theta_0\cos\theta_n\right] \quad (17)$$

where (θ_0, φ_0) is the desired steering angle.

The detailed array configuration can be found in [18]. Nevertheless, in this communication the element spacing has been changed to 0.65 wavelength to reduce the coupling effect, and experimental results reveal that the array gain has been greatly improved.

C. Pattern Synthesis

For conformal arrays, it is common to select the phase to focus the beam in the desired direction. Thus we only take the amplitude weights as optimization parameters. With the phase weights calculated in advance according to (17), the specified scan angle can be guaranteed. However, it should be noted that for some other synthesis problems when the maximum directivity is not sought after, the phases of the elements should also be optimized. Now considering that the optimization for excitation amplitude of each element on the spherical phased array may be a prohibitive task in practice, a previously proposed modified Bernstein polynomial for arc arrays [17] is used to synthesize conformal arrays. The modified Bernstein polynomial is defined as

$$F(U) = \begin{cases} B_1 + \frac{1-B_1}{A^{N_0 A}(1-A)^{N_0(1-A)}} \\ \quad \times U^{N_0 A}(1-U)^{N_0(1-A)}, & 0 \leq U \leq A \\ B_2 + \frac{1-B_2}{A^{N_1 A}(1-A)^{N_1(1-A)}} \\ \quad \times U^{N_1 A}(1-U)^{N_1(1-A)}, & A \leq U \leq 1 \end{cases} \quad (18)$$

where B_1, B_2, M_1, M_2 and A are the parameters in the polynomial. By definition it can be deduced that the modified Bernstein polynomial does not have any oscillations, a common drawback of which always exists in the output of many optimizations and curve fitting routines. With the help of modified Bernstein polynomial, only five variables in our example need to be optimized for each concentric ring, and one variable for the top layer which only consists of only one element. That is to say, for a spherical conformal array consisting of N concentric circular arrays, the total number of variables to be optimized is reduced to $5 \times N + 1$, which significantly reduces the overhead of the optimization.

For the spherical conformal array mentioned above, the cost function to be minimized is defined as the arithmetic mean of the squares of the excess far field magnitude above the specified level. By applying rotations of the local co-ordinate system to the simulated polarized embedded individual radiation pattern located in the $\varphi = 0^\circ$ direction on each concentric ring, radiation patterns of the other elements on the same ring can be determined. Hence, the total field can be obtained by a coherent summation of radiation patterns of each patch in the array. By virtue of using a modified Bernstein polynomial, only 41 variables are optimized for the pattern synthesis of the entire spherical array. In

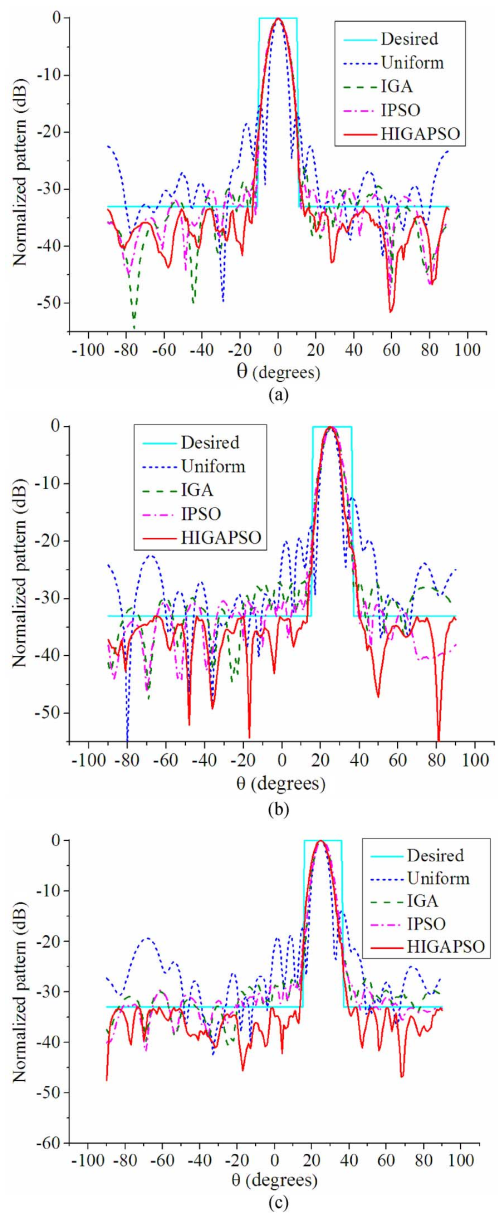

Fig. 4. Radiation pattern for the conformal array after rotation. (a) Scan direction of $(0^\circ, 0^\circ)$. (b) Scan direction of $(25^\circ, 0^\circ)$. (c) Scan direction of $(25^\circ, 45^\circ)$.

addition, the design target is to have a scan range of -25° to 25° from broadside and a side-lobe level of -33 dB or lower.

The improved algorithms (IGA, IPSO and HIGAPSO) are applied to synthesize the far field radiation patterns. The SGA and PSO are not shown because they are inefficient to perform optimization for this case. Parameters are selected the same for these three algorithms to have a fair comparison. Each run has been conducted with a population of 32 individuals and a maximum iteration of 2000. The rest parameters are selected the same as those in the test function. Fig. 4 shows the normalized absolute $\varphi = 0^\circ$ plane radiation pattern in dB for three scan directions of $(0^\circ, 0^\circ)$, $(25^\circ, 0^\circ)$, $(25^\circ, 45^\circ)$, respectively. From the results, it can be seen that the optimization results achieved by HIGAPSO satisfy with the requirements while imperfect results are obtained by either IPSO or IGA. Note that the side-lobe levels in other directions are not optimized and the side-lobes in these directions can be higher.

TABLE I
PERFORMANCE COMPARISONS OF DIFFERENT ALGORITHMS

Scan angle	Uniform		IGA	
	$MSLL_{(dB)}$	N_f	$MSLL_{(dB)}$	N_f
(0°,0°)	-15.2502	——	-26.0814	32768
(25°,0°)	-12.2537	——	-26.6971	33024
(25°,45°)	-13.8894	——	-27.0666	33984
Scan angle	**IPSO**		**HIGAPSO**	
	$MSLL_{(dB)}$	N_f	$MSLL_{(dB)}$	N_f
(0°,0°)	-28.9542	32384	-33.0179	11552
(25°,0°)	-25.2916	32704	-33.0898	13824
(25°,45°)	-28.3977	34304	-33.0054	12832

The shape of the main-beam is also not optimized, only the beam-width in the calculated plane is rejected to the same value. Fig. 5 shows the comparison between the radiation patterns obtained by the proposed method and the full wave simulation results from Ansoft HFSS v11.0. The good agreement between those two results validates our method. Besides, the average maximum side-lobe level (MSLL) and cost function evaluations (N_f) of the improved algorithms over 10 independent runs are given in Table I. Obviously the proposed algorithm achieves a lower average maximum side-lobe level at the scan angles with a faster convergence speed. It is worth pointing out that more factors such as side-lobes and cross-polarization component should also be calculated and optimized throughout the visible region, when our method is applied to the practical design process.

IV. CONCLUSION

A novel hybrid evolutionary optimization algorithm is proposed and its application in spherical phased array synthesis is investigated in this communication. The proposed algorithm combines IGA and IPSO to take advantages of both by means of the grafting principle in botany, where IGA and IPSO are introduced to overcome the drawbacks of GA and PSO.

The proposed algorithm is verified by both classical test function and pattern synthesis of a conformal array. These experimental results show that the hybrid algorithm is able to achieve the optimum design for specified design criteria in an effective manner. The accuracy and the robustness of the hybrid algorithm show its potential applications in a wide class of electromagnetic fields.

APPENDIX

The crossover operator in [15] with its four offspring chromosomes are defined as

$$\vec{b}_1 = \begin{bmatrix} b_1^1 & b_2^1 & \cdots & b_n^1 \end{bmatrix} = (\vec{a}_s + \vec{a}_t)/2 \tag{19}$$

$$\begin{aligned} \vec{b}_4 &= \begin{bmatrix} b_1^4 & b_2^4 & \cdots & b_n^4 \end{bmatrix} \\ &= ((\vec{a}_{\max} + \vec{a}_{\min})(1-w) + (\vec{a}_s + \vec{a}_t)w)/2 \end{aligned} \tag{20}$$

$$\begin{aligned} \vec{b}_2 &= \begin{bmatrix} b_1^2 & b_2^2 & \cdots & b_n^2 \end{bmatrix} \\ &= \vec{a}_{\max}(1-w) + \max(\vec{a}_s, \vec{a}_t)w \end{aligned} \tag{21}$$

$$\begin{aligned} \vec{b}_3 &= \begin{bmatrix} b_1^3 & b_2^3 & \cdots & b_n^3 \end{bmatrix} \\ &= \vec{a}_{\min}(1-w) + \min(\vec{a}_s, \vec{a}_t)w \end{aligned} \tag{22}$$

where $\vec{a}_s$ and $\vec{a}_t$ have the same definition as in Section II-A. Without loss of generality, let's take the kth variable x_k of chromosomes for example. Since $w \in [0,1]$, the ranges determined by (20), (21), (22) are $(\min((x_k^{\max} + x_k^{\min})/2, (x_k^s + x_k^t)/2), \max((x_k^{\max} + x_k^{\min})/2, (x_k^s +$

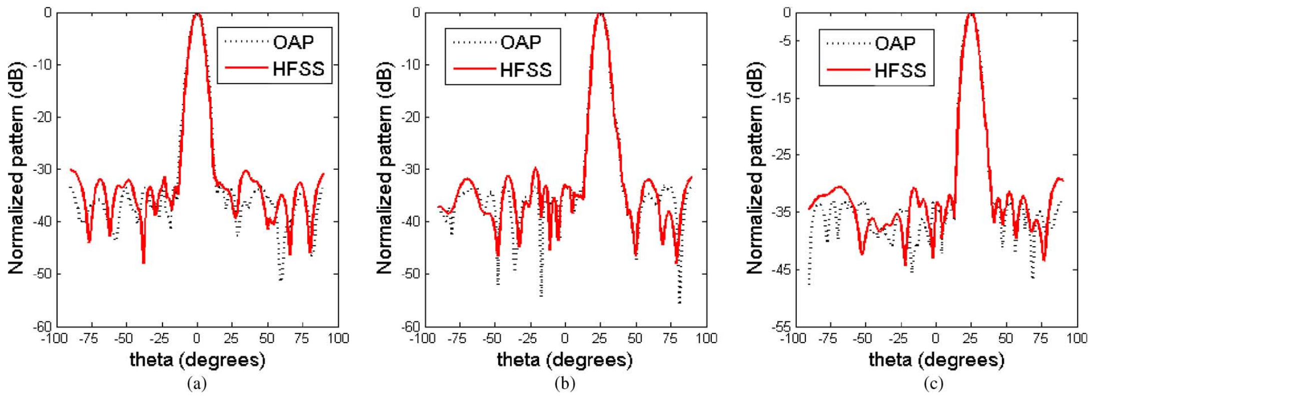

Fig. 5. A comparison of the optimized array pattern (OAP) by the proposed algorithm and the pattern simulated via HFSS. (a) Scan direction of $(0°, 0°)$. (b) Scan direction of $(25°, 0°)$. (c) Scan direction of $(25°, 45°)$.

$x_k^t)/2))$, $(\max(x_k^s, x_k^t), x_k^{\max})$ and $(x_k^{\min}, \min(x_k^s, x_k^t))$, respectively. Actually, some of the search ranges are missed by this crossover operator. Concretely speaking, three cases corresponding to different relationships between $(x_k^{\max} + x_k^{\min})/2$ and $(x_k^s + x_k^t)/2$ can be divided to illustrate this point.

a) If $(x_k^s + x_k^t)/2 < (x_k^{\max} + x_k^{\min})/2$, the range $(\min(x_k^s, x_k^t), (x_k^s + x_k^t)/2)$ is missed.
b) If $(x_k^s + x_k^t)/2 > (x_k^{\max} + x_k^{\min})/2$, the range $((x_k^s + x_k^t)/2, \max(x_k^s + x_k^t))$ is missed.
c) If $(x_k^s + x_k^t)/2 = (x_k^{\max} + x_k^{\min})/2$, the range $(\min(x_k^s, x_k^t), \max(x_k^s + x_k^t))$ is missed, except the point $(x_k^s + x_k^t)/2$.

Therefore, there are certain blind ranges where the offspring can not reach. However, for our proposed crossover, such blind ranges do not exist because the ranges determined by (2) and (3) are $((x_k^s + x_k^t)/2, \max(x_k^s + x_k^t))$ and $(\min(x_k^s, x_k^t), (x_k^s + x_k^t)/2)$, respectively. Therefore, the entire domain can be searched by the offspring.

REFERENCES

[1] C. Dohmen, J. W. Odendaal, and J. Joubert, "Synthesis of conformal arrays with optimized polarization," *IEEE Trans. Antennas Propag.*, vol. 55, no. 10, pp. 2922–2925, Oct. 2007.
[2] L. I. Vaskelainen, "Constrained least-squares optimization in conformal array antenna synthesis," *IEEE Trans. Antennas Propag.*, vol. 55, no. 3, pp. 859–867, Mar. 2007.
[3] K. Wincza, S. Gruszczynski, and K. Sachse, "Conformal four-beam antenna arrays with reduced sidelobes," *Electron. Lett.*, vol. 44, no. 3, pp. 174–175, 2008.
[4] T. E. Morton and K. M. Pasala, "Pattern synthesis of conformal arrays for airborne vehicles," in *Proc. IEEE Aerosp. Conf.*, 2004, vol. 2, pp. 1030–1038.
[5] M. Bucci, A. Capozzoli, and G. D'Elia, "Power pattern synthesis of reconfigurable conformal arrays with near-field constraints," *IEEE Trans. Antennas Propag.*, vol. 52, no. 1, pp. 132–141, Jan. 2004.
[6] P. Knott, "Antenna modeling and pattern synthesis method for conformal antenna arrays," in *Proc. IEEE Antennas and Propagation Society Int. Symp.*, Jun. 2003, vol. 1, pp. 800–803.
[7] B. h. Wang, L. q. Meng, and Y. Guo, "Pattern synthesis of double-curved conformal paraboloidal array," in *Proc. IEEE Antennas and Propagation Society Int. Symp.*, Jul. 2008, pp. 1–4.
[8] P. Paul, F. G. Guimaraes, D. Nair, and D. A. Lowther, "A clonal selection algorithm with varying order finite elements for the optimization of microwave devices," *Microwave Opt. Technol. Lett.*, vol. 50, no. 5, pp. 1392–1397, May 2008.
[9] S. Selleri, M. Mussetta, P. Pirinoli, R. E. Zich, and L. Matekovits, "Differentiated meta-PSO methods for array optimization," *IEEE Trans. Antennas Propag.*, vol. 56, no. 1, pp. 67–75, Jan. 2008.
[10] F. J. Villegas, "Parallel genetic-algorithm optimization of shaped beam coverage areas using planar 2-D phased arrays," *IEEE Trans. Antennas Propag.*, vol. 55, no. 6, pp. 1745–1753, Jun. 2007.
[11] S. M. Mikki and A. A. Kishk, "Hybrid periodic boundary condition for particle swarm optimization," *IEEE Trans. Antennas Propag.*, vol. 55, no. 11, pp. 3251–3256, Nov. 2007.
[12] J. Robinson, S. Sinton, and Y. Rahmat-Samii, "Particle swarm, genetic algorithm, and their hybrids: Optimization of a profiled corrugated horn antenna," in *Proc. IEEE Int. Symp. on Antennas Propagation*, Jun. 16–21, 2002, vol. 1, pp. 314–317.
[13] C.-F. Juang, "A hybrid of genetic algorithm and particle swarm optimization for recurrent network design," *IEEE Trans. Syst., Man, Cybern.-Part B: Cybern.*, vol. 34, no. 2, pp. 997–1006, Apr. 2004.
[14] F. Grimaccia, M. Mussetta, and R. E. Zich, "Genetical swarm optimization: Self-adaptive hybrid evolutionary algorithm for electromagnetics," *IEEE Trans. Antennas Propag.*, vol. 55, no. 3, pp. 781–785, Mar. 2007.
[15] F. H. F. Leung, P. K. S. Tam, H. K. Lam, and S. H. Ling, "Tuning of the structure and parameters of a neural network using an improved genetic algorithm," *IEEE Trans. Neural Networks*, vol. 14, no. 1, pp. 79–88, Jan. 2003.
[16] D. W. Boeringer and D. H. Werner, "Particle swarm optimization versus genetic algorithms for phased array synthesis," *IEEE Trans. Antennas Propag.*, vol. 52, no. 3, pp. 771–779, Mar. 2004.
[17] D. W. Boeringer and D. H. Werner, "Efficiency-constrained particle swarm optimization of a modified Bernstein polynomial for conformal array excitation amplitude synthesis," *IEEE Trans. Antennas Propag.*, vol. 53, no. 8, pp. 2662–2673, Aug. 2005.
[18] W. T. Li, S. F. Liu, X. W. Shi, and Y. Q. Hei, "Low-sidelobe pattern synthesis of spherical array using the hybrid genetic algorithm," *Microwave Opt. Technol. Lett.*, vol. 51, no. 6, pp. 1487–1491, Jun. 2009.